

REF: Final Report (Year 4) – Andrew Fellowship – IChemE

DATE: 29th March 2019

1. Main scope of this fellowship work.

To grow carbon nanotube forests with controlled chirality.

2. Background.

Carbon nanotubes (CNTs) are an allotrope of carbon. They are hollow structures that can be viewed as rolled-up sheets of graphene (a two dimensional crystal of honeycomb-arranged carbon atoms). If the tubes are formed by just one graphene sheet, they are referred as single-walled nanotubes (SWNTs), otherwise as multi-walled tubes. SWNT diameters typically range from ~0.8 to up to 3 nm and that is equivalent to just a few carbon atoms. The arrangement of the atoms along the longitudinal axis of the tube is called chirality and dictates their electrical properties. Nanotube chirality cannot yet be controlled during the synthesis and has been the objective of this four-year fellowship work.

CNTs are typically synthesised by the chemical vapour deposition (CVD) method, and can grow in tangled mats or vertically aligned to a substrate in an arrangement denominated forests. The alignment arises from a particular catalyst–support interaction in which the particles remain bound to the support material during the CVD process. The quintessential catalyst–support system to grow forests is alumina–Fe. Forest synthesis includes two main steps: catalyst preparation and growth itself.

The catalyst is prepared by restructuring a thin film of a transition metal (typically Ni, Co, or Fe) into nanoparticles. This is done at temperatures ranging between 500 and 800 °C in a reducing atmosphere (H₂ or NH₃ - mbar to bar range) to de-oxidise (and hence activate) the particles. The density, size, and size distribution of the nanoparticles are strongly correlated to the thickness of the film, the temperature of the process, and the catalyst support, among other parameters.

To nucleate and grow the tubes, nanoparticles are exposed to a carbon-containing gas. The molecules of the gas dissociate at the catalyst surface and carbon atoms dissolve into the nanoparticles until reaching saturation. This leads to a cap formation at the exposed areas of the nanoparticles and subsequently to tube growth. The resulting diameter, number of walls, and chirality of the tubes strongly depend on the catalyst size. SWNTs require catalyst particles no larger than one nanometre in projected diameter.

3. Summary of work and achievements.

Until now nanotube synthesis has been unable to yield tubes with specific properties mainly because the growth mechanism is not fully understood and it remains unclear what reaction parameters dictate the arrangement of carbon atoms. Throughout the fellowship period the reaction has been studied in detail and, although full control has not been achieved, the following has been accomplished, as follows:

3.1 Enrichment of chirality (from 35 to 7) using typical catalysts Fe or Fe-Co.

3.2 Low temperature growth using Fe only.

- 3.3 Identification of a new catalyst system Co-Nb to lower the growth temperature.
- 3.4 Identification of temperature as the most critical parameter for controlling the reaction.
- 3.5 Determination of minimum thickness to grow a forests.
- 3.6 Understanding the reason chirality fluctuates even with same-diameter particles.
- 3.7 Understanding that chirality control cannot be achieved by vapour-phase deposited catalysts.
- 3.8 Enrichment of chirality using plasma-treated, continuous Co-W films.

3.1 Chirality enrichment.

It is achieved for the first time forest growth with just seven different chiral angles using Fe-Co bimetallic catalyst.

The starting point of this research is the state-of-art catalyst system (Fe-coated Al_2O_3) and optimised growth conditions (see Table 1, standard catalyst). This delivers millimetre-range forests with a reproducible number of chiralities, varying from 35 to 41. For the best-result samples, the ratio semiconducting to metallic tubes is roughly 4:1. The chiral angles and the abundance vary from sample to sample. A set of 22 samples is evaluated (Table 2).

The first strategy to control chirality is to assess bimetallic catalysts for alloys have been regarded as chirality enhancers. Fe-Co is studied in depth. By combining ultra-thin films of Fe and Co, the growth temperature is reduced from 750 to 480 °C (Table 1, Fe-Co catalyst). The number of chiralities is narrowed from 40 to 7 (Table 3). The ratio between semiconducting and metallic tubes is similar to that at high temperature; again, the actual chiral angles and their abundance vary from sample to sample (see Table 4 and Figure 1). Density functional theory calculations indicate Fe-Co is a faster catalyst than Fe or Co, as the carbon solubility in the Fe alloy increases from 0.031 to 0.057 atomic % and the carbide heat of formation per C atom from 0.08 to 0.22 eV. Although this is far from nanotube chirality control, the results suggest alloys are a promising route.

3.2 Lowest ever growth temperature.

It is achieved reproducible forest growth at a temperature as low as 375 °C using Fe mono-catalyst.

Temperature is key parameter in CNT CVD. Lowering temperature is a means to control catalyst size and size distribution. Two factors are critical to enforce low temperature growth: use of ammonia and low carbon source partial pressure. Ammonia induces catalyst *austenisation* (i.e. γ -Fe formation). Pure-phase γ -Fe nanoparticles dissolve up to 2.14 % of carbon and evolve to cementite (Fe_3C) phase. Fe_3C facilitates carbon segregation as it is metastable above ~350 °C. In addition, the chamber pressure (C_2H_2 and NH_3) must not exceed 5×10^{-2} mbar. Higher pressures induce Fe catalyst poisoning. Nanoparticles deactivate as carbon diffusivity, and hence mobility, dramatically diminish using low temperature (diffusivity scales with temperature, according to $\exp[-AG/T]$). (Growth conditions in Table 1, Low T system). Chirality assignment reveal 7 to 9 chiralities (similar to the Fe-Co case), so no real need of bi-metallic catalysts (see data in Table 5). This is a better option as a single catalyst eliminates one variable.

3.3 Identification of a new catalyst system Co-Nb to lower the growth temperature.

It is identified a new catalyst system, Co-Nb, that allows reproducible forest growth at a record low temperature of 325 °C.

Several Co-based catalyst systems are evaluated by alloying ultra-thin films of Co with high melting point metals (including W, Ta, Nb, Ir, and Pt). The best results are obtained for the Co-Nb system as forest growth is reproducible at 325 °C (Table 1, Co-NB catalyst). This can be attributed to a faster reduction of Co. X-ray photoemission spectroscopy (XPS) has shown that Co reduces at lower temperatures when in the presence of Nb. This is similar to Co alloyed with Mo, with the advantage that the actual growth temperature is much lower 325 instead of 800 °C. It remains unclear whether Nb

catalyses the reaction or just enhances Co reduction. In purely metallic state, it does not induce nanotube growth. Chirality assignment shows, for the best samples, a maximum of 8 chiral angles: 3 metallic (37.5%) and 5 semiconducting (62.5%), Table 6. Hence, chirality enrichment appears to have reached saturation as three different catalyst systems display similar results.

3.4 Identification of *temperature* as the most critical parameter to control the reaction.

It is identified temperature as the most critical parameter to control the reaction and reproducibility.

One of the main difficulties on controlling chirality is the lack of understanding of the nanotube growth mechanism. It is well known that controlled growth requires homogeneously-sized nanoparticles and predefined growth conditions, but the reproducibility is a major issue. To overcome this, the main strategy is to reduce as much as possible the size of the particles, to find the lowest growth temperature, and to adjust the growth conditions to each catalyst system.

Once optimal synthesis conditions are found for a catalyst system (e.g. Fe-Co) in a growth chamber, they are repeated in different CVD systems. Unexpectedly, chirality assignment reveals dramatic differences (Table 7), which can only be attributed to temperature oscillation amongst chambers. Further investigation reveals that a variation of just ~3% from the temperature set up (typical for a CVD system) is critical to particle size and density, particle surface diffusion, and catalyst activity. It is therefore challenging to reproduce chirality results when changing growth systems as the reaction is extremely sensitive to slight variations of temperature.

3.5 Identification of minimum thickness to grow a forest.

It is identified that the minimum thickness to grow a forest is nominal 0.3 nm of Fe.

Typical SWNT diameters range from ~0.6 to ~1.5 nm and are seeded by nanoparticles obtained by restructuring metal thicknesses of ~1nm or below. This diameter range also gives about 180 different chiral angles, so it is absolutely necessary to produce uniform catalysts; one of the means to achieve this is to reduce the starting catalyst thickness. It is systematically reduced until found that nominal 0.3 nm of catalyst is the limit to induce forest growth; 0.1 or 0.2 nm thicknesses yield just low-density disordered tubes. The size of the particles obtained by 0.3 nm Fe, as estimated from atomic force microscope images (using jpeg software), is 1.15 ± 0.05 nm, Figure 2.

3.6 Understanding the reason chirality fluctuates even with same-diameter particles.

It is thoroughly analysed the dynamics of the catalyst and determined that undergoes dramatic variations during both nucleation and growth periods, critical to chirality control.

In order to understand the temperature effect and get insight into the growth mechanism, it is performed in-situ high-resolution transmission electron microscopy. It is observed that, upon supply of the carbon source into the growth chamber, the nanoparticles diffuse across the support, merge into larger particles (i.e. clustering, Figures 3a-3b), and eventually nucleate large/defective tubes (Figure 3c). The dynamics of the catalyst are also observed at the atomic level. It is seen reshaping of the catalyst with increasing of contact metal/segregated layers of carbon, especially at the early stage of growth (Figures 3d-3e). As a result, the tubes change their diameter which induces various arrangements of carbon atoms and hence different chiral angles.

3.7 Identification of limits imposed by vapour-deposited thin films.

It is understood that restructuring of thin films to form catalyst nanoparticles inflicts homogeneity limitations so that chirality control is unachievable using this catalyst formation strategy.

In section 5 it is reported that the minimum thickness to grow a forest is nominal 0.3 nm of Fe. Such ultra-thin films are non-continuous and induce the formation of nanoparticles very homogenous in size and size distribution. Using optimised growth conditions –including the lowest possible growth temperature– these particles steadily deliver between 7 and 10 different chiral angles per sample, and it appears to be more than extremely challenging to achieve further improvement. This suggests

nanoparticles formed via restructuring of vapour-deposited metal films have reached their limit of efficiency. The essential level of narrowness in catalyst size and size distribution requires nanoparticle control at the very atomic level. That exceeds the limits offered by the physical deposition methods so different preparation strategies might be necessary (such as fine chemistry or continuous catalyst films). Fine chemistry, for instance, may offer better control of the catalyst, perhaps the necessary one to produce nanoparticles with exactly the same number of atoms and same crystallographic structure. Even if there are small variations (whether in particle formation or growth process), in principle, chirality could be further enriched.

Figure 2 shows one of the best particle size distribution for Fe. Although the size dispersion appears to be very narrow (1.15 ± 0.05 nm, as theoretically estimated using jpeg software), it is still too large for the purpose of chirality control. The reason is that the catalyst not only decomposes the carbon source/enforces carbon segregation, but also acts as template for tube formation. Any difference in nanoparticle size, even if small, has a great impact on carbon atomic arrangement.

3.8 Chirality enrichment using large catalyst particles and continuous films.

It is achieved ~70% of single-chirality, metallic-type tubes per sample using plasma-treated, continuous, thick W-Co films.

Having identified the limitations encountered on restructuring thin films, a new strategy is evaluated: nanotube growth using micro-meter size nanoparticles. Large particles are expected to remain in solid state so that surface diffusion, clustering, and reshaping be minimised or inexistent. Following long annealing times, large particles undergo faceting which, upon low dosage of carbon source, nucleate small-diameter tubes at energetically favourable facets. It is expected that chirality should be the same for all tubes, but this is challenging to assess as Raman spectroscopy encounters interference from large metallic particles as well as other forms of carbon present.

Nevertheless, the principle is used to grow carbon nanotubes from Co-W continuous films subjected to plasma treatment (Table 1 Co-W catalyst). It is observed growth across large areas of the samples, on all evaluated samples, with tubes lying on the surface; vertical alignment has not been achieved as the tube area density is much lower than that of a forest (Figure 4a). Chirality assignment reveals three different chiralities 2 semiconducting-, 1 metallic-type (Figures 4b-4c). The metallic tubes consist of the (12,6) structure and its highest abundance is found to be ~68% Figure 4d). The tubes are larger in diameter than those synthesised via film-restructured catalysts which is attributed to growth from slabs rather than particles. Variations in the plasma treatment give no significant improvement of the yield to the extent of no growth for long time treatments. It remains unclear whether just one metal (W or Co) or the alloy is the actual catalysts. On the catalyst preparation, it has been observed a eutectic point so the carbon solubility might be increased at that temperature/composition making the slabs very catalytically active. This warrants further investigation. Finally, these results are in good agreement with a previous work (Yang et al. Nature 510, 522 2014). Advantageously, thick Co-W catalyst films can be prepared at wafer scale so they may find industrial applications once the reaction is fully controlled.

4. Conference presentations.

(1) Growth of carbon nanotubes with enriched chiral angles.

S Esconjauregui, L D'Arsie, H. Sugime, R Xie, Y Guo, J Robertson.

UKCC 19, Manchester, UK January 2019. Oral presentation.

(2) Carbon nanotube forest growth at 375 °C: process decoupling and temperature effect on chirality distribution.

S Esconjauregui, L D'Arsie, H. Sugime, R Xie, Y Guo, J Robertson.

NT 18, Beijing, China. July 2018. Oral presentation.

(3) Towards the growth of carbon nanotubes with controlled chirality.

S Esconjauregui, L D'Arsie, H. Sugime, R Xie, Y Guo, J Robertson.
UKCC 18, Manchester, UK January 2018. Oral presentation.

(4) Low temperature growth of carbon nanotube forests with enriched chirality.

S Esconjauregui, L D'Arsie, H. Sugime, R Xie, Y Guo, J Robertson.
NT 17, Belo Horizonte, Brazil. June 2017. Oral presentation.

(5) Doping of carbon nanotubes forests by MoO₃.

S Esconjauregui, L D'Arsié, J Robertson.

31st International winter school on electronic properties of novel materials. Kirschberg, Austria. March 2017. Poster presentation.

(6) Evaluation of bimetallic catalysts for the growth of carbon nanotube forests.

S Esconjauregui, R Xie, Y Guo, J Robertson.

Material Research Society Fall Meeting 2015, Boston, US, December 2015. Oral presentation.

5. Publications.

(1) Low temperature growth of carbon nanotube forests with enriched chirality.

S Esconjauregui, L D'Arsie, H Sugime, R Xie, Y Guo, J Robertson.

Manuscript status: finished, co-author review.

(2) In-situ TEM observation of nanotube catalysis: effect of temperature and carbon source on chirality

S Esconjauregui, L D'Arsie, Y Guo, J Robertson.

Manuscript status: in preparation (TEM analysis finished, XPS analysis missing).

(3) Bi-metallic catalyst for controlled nanotube growth.

S Esconjauregui, Y Guo, J Robertson.

Manuscript status: in preparation (Raman analysis finished, DFT calculations finished, HRTEM missing).

6. Conclusions and future work.

Over four years of research on chirality control, it has been thoroughly studied the growth mechanism of nanotubes and managed to narrow the number of chiral angles in a forest down to just seven (without a clearly defined tendency in abundance). This appears to be the limit for catalyst nanoparticles prepared by restructuring thin films, regardless of the employed metal(s) and the evaluated growth conditions.

The best results, by contrast, are achieved on plasma-treated, continuous Co-W films. This yields low-density tubes with nearly 70% of same metallic-type chirality. Such results pave the way to further studies in chirality control using similar catalyst preparation strategy. Further studies on W-Co system will ensure reproducibility, understanding on the catalyst composition, and eventually industrial applications.

On the basis of the results obtained over four years of this fellowship work, I will be asking further funding to continue working on chirality-specific growth of nanotubes.

Case of Study	Support	Catalyst	Pre-treatment	Growth
Standard catalyst	Si/10 nm Al ₂ O ₃	0.3-0.5 nm Fe	750 °C, H ₂	H ₂ , C ₂ H ₂
Fe-Co catalyst	Si/10 nm Al ₂ O ₃	0.3 nm Fe-Co	480 °C, H ₂	H ₂ , (NH ₃), C ₂ H ₂
Low T system	Si/10 nm Al ₂ O ₃	0.3 nm Fe	375 °C, NH ₃	NH ₃ , C ₂ H ₂
Co-Nb catalyst	Si/10 nm Al ₂ O ₃	0.4 nm Co-Nb	325 °C, NH ₃	NH ₃ , C ₂ H ₂
Co-W catalyst	Si/10 nm Al ₂ O ₃	50,100 nm Co-W	*1050 °C, NH ₃	NH ₃ , (H ₂), CH ₄

Table 1. Main catalyst preparation and growth conditions for the systems studied in this work. (*) denotes plasma treatment prior to growth. Gases in brackets indicate they deliver similar results to other reducing agent.

Sample	Chiral angles	Metallic (Percentage)		Semiconducting (Percentage)	
1	35	9	25.71	26	74.29
2	35	9	25.71	26	74.29
3	35	10	28.57	25	71.43
4	36	12	33.33	24	66.67
5	36	10	27.78	26	72.22
6	37	11	29.73	26	70.27
7	37	9	24.32	28	75.68
8	37	9	24.32	28	75.68
9	38	13	34.21	25	65.79
10	39	13	33.33	26	66.67
11	39	12	30.77	27	69.23
12	39	11	28.21	28	71.79
13	40	14	35.00	26	65.00
14	40	14	35.00	26	65.00
15	40	12	30.00	28	70.00
16	40	12	30.00	28	70.00
17	40	11	27.50	29	72.50
18	41	14	34.15	27	65.85
19	41	13	31.71	28	68.29
20	41	12	29.27	29	70.73
21	41	12	29.27	29	70.73
22	41	10	24.39	31	75.61

Table 2. Chirality assignment using standard growth conditions (for reference).

Sample	Chiral angles	Metallic (Percentage)		Semiconducting (Percentage)	
1	7	3	42.86	4	57.14
2	7	2	28.57	5	71.43
3	7	2	28.57	5	71.43
4	7	2	28.57	5	71.43
5	7	1	14.29	6	85.71
6	7	1	14.29	6	85.71
7	7	1	14.29	6	85.71
8	8	3	37.50	5	62.50
9	8	3	37.50	5	62.50
10	8	2	25.00	6	75.00
11	8	2	25.00	6	75.00
12	8	2	25.00	6	75.00
13	9	3	33.33	6	66.67
14	9	3	33.33	6	66.67
15	9	2	22.22	7	77.78

Table 3. Chirality assignment using Fe-Co catalyst.

TUBE	DIAM (nm)	SAMPLE 1		SAMPLE 2		SAMPLE 3		SAMPLE 4	
		SC	M	SC	M	SC	M	SC	M
	0.88								
7,6	0.89							20	
8,5	0.90		8		6				14
	0.91								
9,4	0.92	7		5				10	
	0.93								
10,3	0.94	31		17		15		13	
	0.95								
	0.96								
	0.97								
9,5	0.98	3						24	
12,1	0.99	3		14		7		5	
10,4	1.00		11		9		11		9
11,3	1.01	11				9			
	1.02								
	1.03								
12,2	1.04	14							
10,5	1.05	12		10		17			
	1.06								
11,4	1.07			22		26			
13,1	1.08				17				5
12,3	1.09						15		
	1.10								

Table 4. Chirality count for four samples using Fe-Co catalyst.

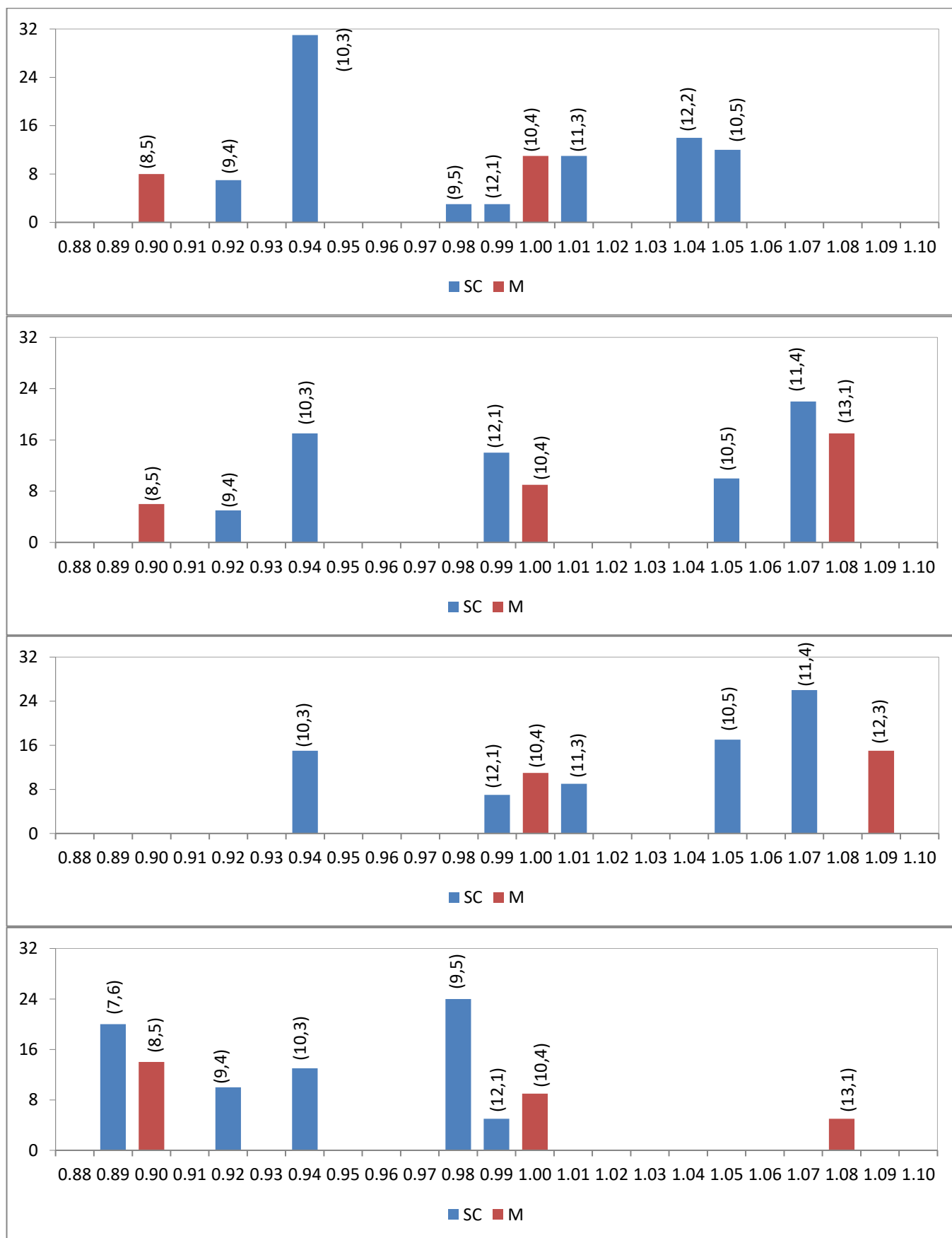


Figure 1. Chirality abundance for four samples using Fe-Co catalyst as described in Table 4 (sample 1 to sample 4, top to bottom, respectively).

Sample	Chiral angles	Metallic (Percentage)		Semiconducting (Percentage)	
1	7	2	28.57	5	71.43
2	7	2	28.57	5	71.43
3	7	1	14.29	6	85.71
4	8	3	37.50	5	62.50
5	8	2	25.00	6	75.00
6	8	2	25.00	6	75.00
7	8	2	25.00	6	75.00
8	9	4	44.44	5	55.56
9	9	3	33.33	6	66.67
10	9	3	33.33	6	66.67

Table 5. Chirality assignment using pure Fe catalyst and low temperature growth.

Sample	Chiral angles	Metallic (Percentage)		Semiconducting (Percentage)	
1	8	3	37.50	5	62.50
2	8	2	25.00	6	75.00
3	9	3	33.33	6	66.67
4	9	3	33.33	6	66.67
5	9	2	22.22	7	77.78
6	10	4	40.00	6	60.00
7	10	3	30.00	7	70.00
8	10	3	30.00	7	70.00
9	10	3	30.00	7	70.00
10	11	3	27.27	8	72.73

Table 6. Chirality assignment using Co-Nb catalyst.

SAMPLE	GROWTH	CVD SYSTEM	PLACE	CHIRALITY RESULTS		
				ANGLES	MET	SC
Sample 1 500 C	G1	Black Magic	CAM	7	2	5
	G2	(Plasma) Cold Wall	CAM	8	4	4
	G3	Black Magic 3	DEL	11	4	7
	G4	Cold Wall	UPM	9	3	6
	G5	Black Magic	CAM	12	4	8
	G6	(Plasma) Cold Wall	CAM	9	2	7
	G7	Black Magic 3	DEL	7	2	5
	G8	Cold Wall	UPM	14	5	9
Sample 2 480 C	G9	Black Magic	CAM	10	3	7
	G10	(Plasma) Cold Wall	CAM	16	5	11
	G11	Black Magic 3	DEL	12	3	9
	G12	Cold Wall	UPM	8	3	5
	G9	Black Magic	CAM	8	2	6
	G10	(Plasma) Cold Wall	CAM	11	4	7
	G11	Black Magic 3	DEL	9	3	6
	G12	Cold Wall	UPM	8	2	6
Reference (750 C)		Cold wall	CAM	35	9	26

Table 7. Chirality assignment for two samples using same growth setting parameters on different growth chambers.

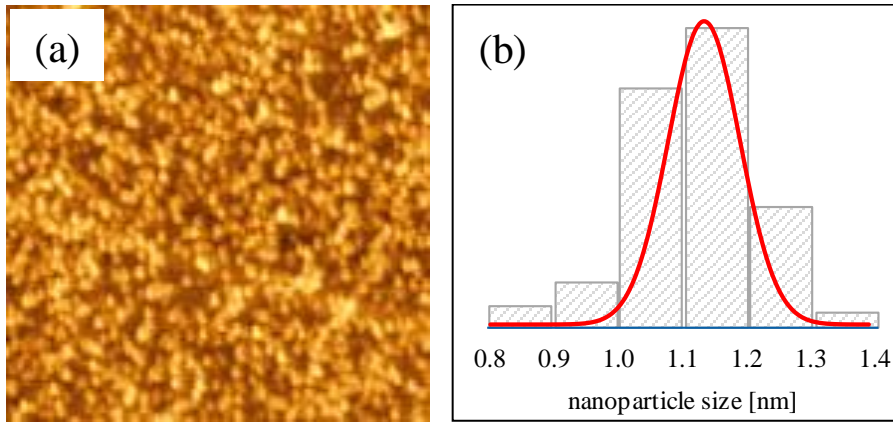


Figure 2. (a) AFM image of catalyst nanoparticles and (b) calculated size distribution.

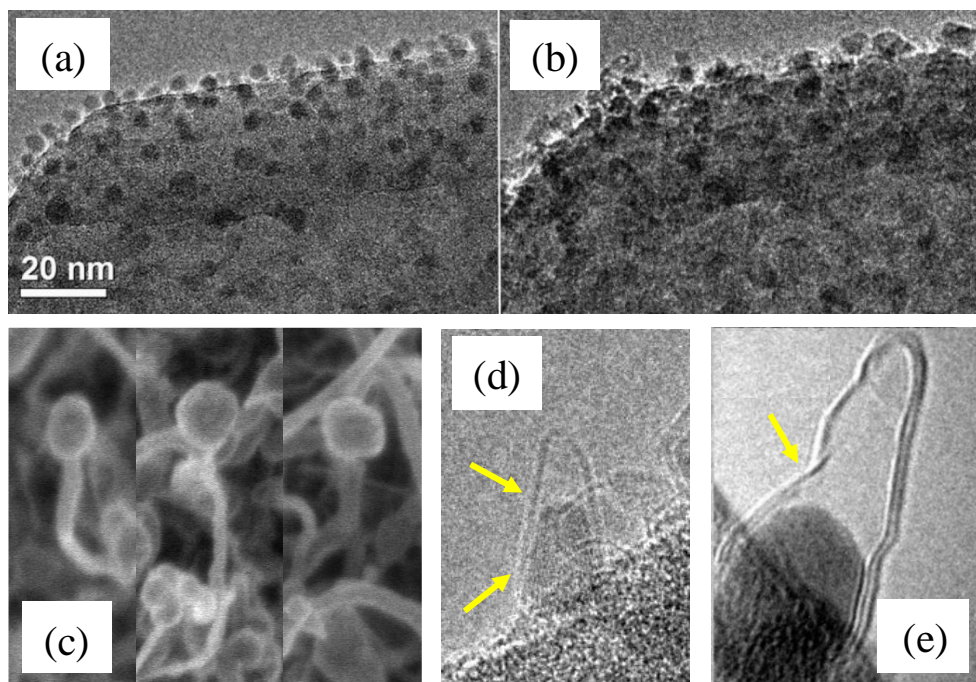
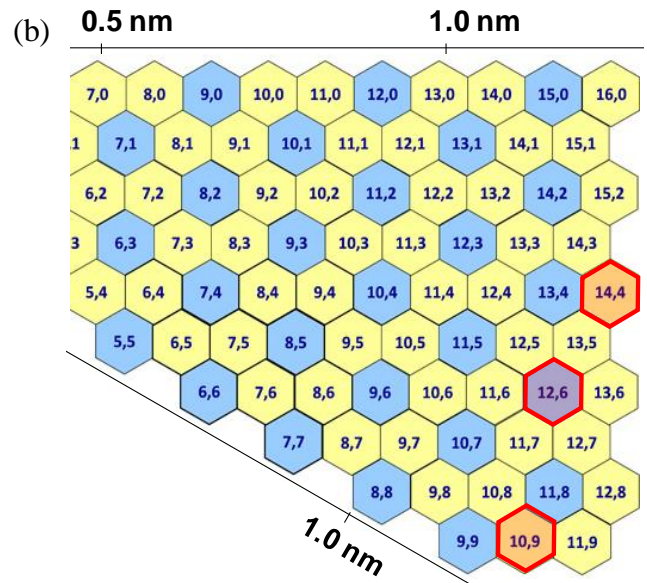
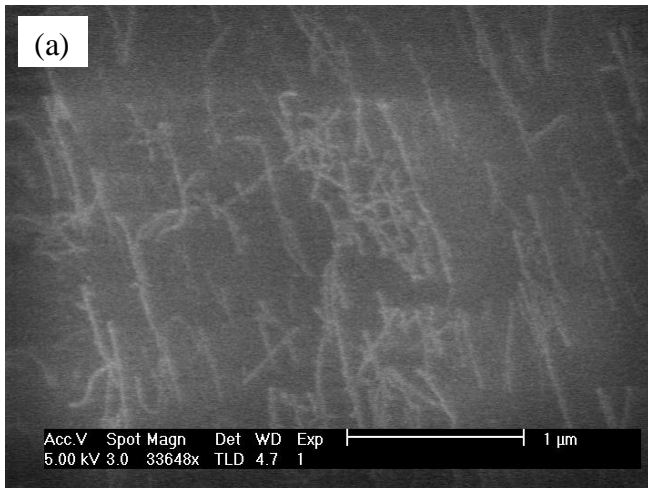


Figure 3. (a-b) HRTEM images of catalyst nanoparticles before and after carbon source supply. (b) SEM images of tubes seeded by clusters of nanoparticles after sintering. (d-e) HRTEM images of catalyst particles wetting the tubes and creation of defects as a result (arrow indication).



(c)

TUBE	DIAM (nm)	SAMPLE 1	
		SC	M
(11,7)	1.25		
(12,6)	1.26		36
(16,0)	1.27		
(13,5)	1.28		
(15,2)	1.28		
(14,4)	1.30	12	
(10,9)	1.31	5	
(16,1)	1.31		

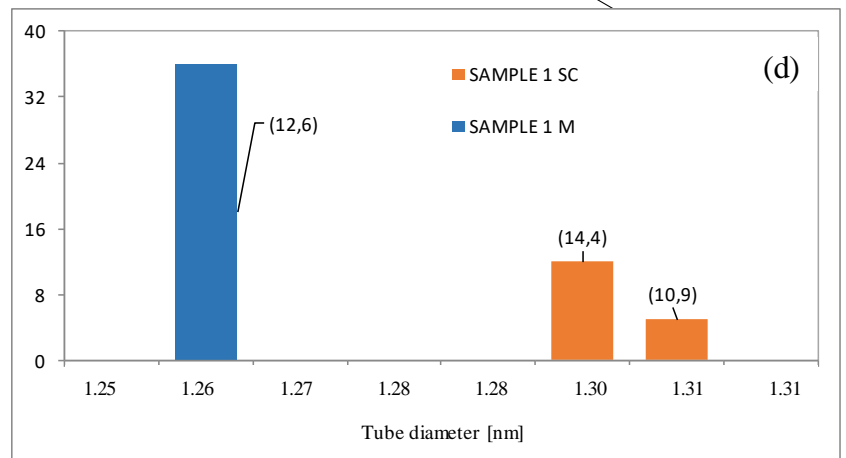


Figure 4. (a) SEM images of tubes grown using Co-W catalyst. (b-c) Chirality assignment and (d) abundance for a sample. This compares to sample analysis shown in Table 4 and Figure 1.

Sample	Chiral angles	Metallic (Percentage)		Semiconducting (Percentage)	
1	3	1	33.33	2	66.66
2	3	1	33.33	2	66.66
3	4	1	25.00	3	75.00
4	4	2	50.00	2	50.00
5	4	1	25.00	3	75.00
6	5	2	40.00	3	60.00

Table 8. Chirality assignment for six samples using Co-W catalyst system. Abundance is estimated for sample 1 only (as described in Figure 4).